Modification of Δ′ by magnetic feedback and kinetic effects

Yueqiang Liu, R. J. Hastie, and T. C. Hender

Citation: Phys. Plasmas **19**, 092510 (2012); doi: 10.1063/1.4754281
View online: http://dx.doi.org/10.1063/1.4754281
View Table of Contents: http://pop.aip.org/resource/1/PHPAEN/v19/i9
Published by the American Institute of Physics.

Modification of Δ' by magnetic feedback and kinetic effects

Yueqiang Liu,[a] R. J. Hastie, and T. C. Hender
Euratom/CCFE Fusion Association, Culham Science Centre, Abingdon OX14 3DB, United Kingdom

(Received 24 August 2012; accepted 7 September 2012; published online 24 September 2012)

Two possible ways of modifying the linear tearing mode index, by active magnetic feedback and by drift kinetic effects of deeply trapped particles, are analytically investigated. Magnetic feedback schemes, studied in this work, are found generally stabilizing for Δ'. The drift kinetic effects from both thermal particles and hot ions tend to reduce the power of the large solution from the outer region. This generally leads to a destabilization of Δ' for the toroidal analytic equilibria considered here. [http://dx.doi.org/10.1063/1.4754281]

I. INTRODUCTION

The tearing mode is one of the most important magnetohydrodynamic (MHD) instabilities in fusion devices. In tokamaks, the onset of neoclassical tearing mode (NTM) is one of the major obstacles in achieving high performance, high pressure plasmas,[1] in particular for International Thermonuclear Experimental Reactor (ITER).[2] In reversed field pinch (RFP) devices, simultaneous presence of multiple tearing modes is thought responsible for reaching the force-free configuration. However, passive or active control of these modes may lead to a new regime in RFPs, in which only a single or few tearing mode is unstable, creating a so-called (quasi) single helicity state,[3,4] with significantly improved plasma confinement in certain regions of the plasma.

Theoretically, the tearing mode is conventionally analyzed by separately solving the problem of layer physics near the rational surface, where the plasma inertia, resistivity, and possibly viscosity effects become important, and the problem in the bulk outer region, in which the plasma is normally well described by ideal, single fluid MHD equations.[5] A key parameter, the so-called stability parameter for the tearing mode (or simply tearing mode parameter) Δ',[6] defined as the logarithmic jump of the perturbed radial magnetic field, is derived from the outer solution, which matches to the resistive layer solution to obtain the final dispersion relation for the mode stability. For NTMs, the parameter Δ', being normally negative, plays a key role in determining the magnetic island onset condition and the island evolution, as shown by the generalized Rutherford equation.[7–9] Therefore, mitigation or suppression of tearing modes in many cases can be achieved by reducing (stabilizing) Δ'.

In this work, we consider two possible mechanisms of modifying Δ': one is due to the kinetic effects of energetic particles (the passive way), the other is active control of Δ' using magnetic feedback.

Active control of tearing modes in tokamaks is normally achieved by acting on the tearing layer. One example is the electron cyclotron current drive (ECCD) stabilization of tearing modes, which has been demonstrated both in theory[10–12] and in experiments.[13–15] This is a non-magnetic control scheme. Magnetic control of the tearing mode, by directly controlling the magnetic islands with external fields seems to encounter a difficulty of the so-called phase instability,[16–18] in which the island chain naturally locks to the external resonant field in such a helical phase, which the islands are destabilized. This process is non-linear and is beyond the scope of the present work. In the linear phase, Finn[19] studied the direct active control of the tearing mode growth rate, based on magnetic feedback. In this work, we propose a completely different methodology for the tearing mode control, namely we focus on active control of Δ' using magnetic coils. The results are still applicable for controlling the stability of a linear tearing mode. But since the results do not depend on the inner layer physics, they can also be useful for the NTM study. Our control configuration is also slightly different from that assumed by Finn.

The kinetic effects on the tearing mode stability have been conventionally analyzed for the resistive layer.[20–24] Here, we investigate possible kinetic effects from trapped particles on Δ'. We mention that Cai *et al.*,[25,26] recently studied the kinetic effect of energetic ions on Δ', and concluded that the co-circulating (counter-circulating) energetic ions reduce (increase) Δ', whereas the trapped hot ions destabilize Δ'. For circulating hot ions, it has been shown that the kinetic effect comes from the finite orbit width effect.[25] Similar destabilization effect by energetic particles has also been reported in another numerical study of the tearing mode instability.[27] In this work, we find a destabilizing effect from deeply trapped particles (both thermal ions and electrons as well as hot ions) due to the non-adiabatic drift kinetic response, even neglecting the finite orbit effect. The main physics of destabilization of Δ' comes from the kinetic modification of the Mercier index.

In Sec. II, we study the *linear* modification of Δ' by magnetic feedback control schemes, based on a simple cylindrical geometry and the ideal MHD theory. Various types of active and sensor coils are considered. In Sec. III, we investigate the drift kinetic effects of trapped particles on Δ'. This requires consideration of toroidal geometry. A relatively simple Newcomb-like equation is obtained by considering only deeply trapped particle contribution. Section IV summarizes the results.

II. FEEDBACK MODIFICATION OF Δ'

A. Δ' in the absence of feedback

Here, we focus on capturing the main physics features, by assuming a cylindrical geometry with a single poloidal

[a]E-mail: yueqiang.liu@ccfe.ac.uk.

mode approximation. We consider the well known Newcomb equation with finite plasma pressure[28]

$$\frac{1}{r}\frac{d}{dr}\left(r\frac{d\psi}{dr}\right)-\frac{m^2}{r^2}\psi-\frac{m}{rF}\frac{dJ_z}{dr}\psi-\frac{2m^2B_\theta^2}{r^3B_z^2F^2}\frac{dP}{dr}\psi=0, \quad (1)$$

where r is the radial coordinate along the plasma minor radius. ψ is the m-th poloidal harmonic of the perturbed poloidal magnetic flux function, which has an $\exp(im\theta - ikz)$ variation along the poloidal angle θ and the z-axis, k is the wave number along the z-direction. J_z is the z-component of the equilibrium plasma current density. $F \equiv mB_\theta - kB_z$, where $\mathbf{B} = B_\theta\hat{\theta} + B_z\hat{z}$ is the equilibrium field. P is the equilibrium plasma pressure.

For simplicity, we assume a step function for the current density profile $J_z(r)$, with $J_z = J_0 = const$ at $0 \le r < r_0$, and $J_z = 0$ at $r_0 < r \le a$. a is the plasma minor radius. Following,[19,29] we also assume a constant pressure $P = P_0 = const$ across the whole plasma column, noting meanwhile that this is not a consistent pressure profile satisfying the equilibrium force balance condition. A schematic plot of these equilibrium profiles, as well as that of the safety factor q, is shown in Fig. 1. The q profile is constant for $0 \le r < r_0$, and parabolic for $r_0 < r \le a$. We also assume that a rational surface, with $q(r_s) = m/n$, is located at r_s, between r_0 and a.

With all the above assumptions for radial profiles, Eq. (1) turns into the vacuum equation

$$\nabla_\perp^2\psi \equiv \frac{1}{r}(r\psi')' - \frac{m^2}{r^2}\psi = 0$$

everywhere inside the plasma, except at discrete radial points $r = r_0, r_s, a$, where jump conditions are obtained for the radial derivative of the flux function ψ. Following standard integration techniques, we have (assuming, without loses of generality, $m > 0$)

$$\left.\frac{r[\psi']}{\psi}\right|_{r_0} = -\frac{2m}{m-nq_0}, \quad (2)$$

$$\left.\frac{r[\psi']}{\psi}\right|_{a} = -\frac{\beta m^2}{(m-nq_a)^2}, \quad (3)$$

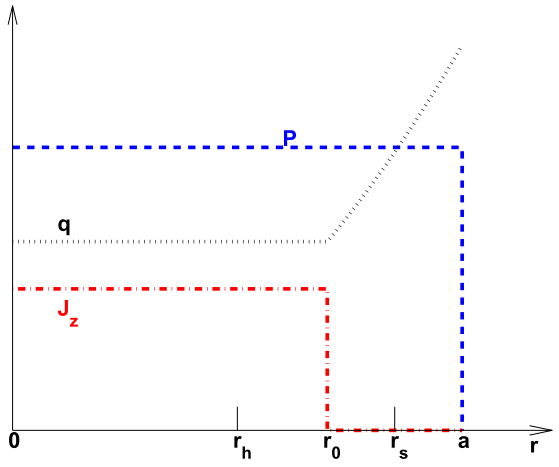

FIG. 1. Sketch of the equilibrium profiles used for calculating Δ' in the presence of magnetic feedback.

where $\beta = 2\mu_0P_0/B_z^2, q_a = q_0(a/r_0)^2$. In the absence of a wall, the above jump conditions, and the conditions $r\hat{\psi}'/\hat{\psi}|_{r_0-} = m$ and $r\hat{\psi}'/\hat{\psi}|_{a+} = -m$, can be connected together, from both sides of the rational surface $r = r_s$, by a relation

$$\frac{1+\frac{1}{m}\frac{r\psi'}{\psi}\Big|_{r_1+}}{1-\frac{1}{m}\frac{r\psi'}{\psi}\Big|_{r_1+}} = \left(\frac{r_1}{r_2}\right)^{2m}\frac{1+\frac{1}{m}\frac{r\psi'}{\psi}\Big|_{r_2-}}{1-\frac{1}{m}\frac{r\psi'}{\psi}\Big|_{r_2-}}, \quad (4)$$

valid between any two points within a "regular" region. This standard procedure eventually yields

$$\Delta' = -\frac{2m}{r_s}\left[\frac{B}{r_s^{2m}/a^{2m}+(1-r_s^{2m}/a^{2m})B} - \frac{A}{r_s^{2m}/r_0^{2m}+(1-r_s^{2m}/r_0^{2m})A}\right], \quad (5)$$

where

$$B = 1-\frac{m\beta}{2(m-nq_a)^2}, \quad A = \frac{1}{m-nq_0}.$$

In order to slightly generalize the above calculations, we introduce a thin resistive wall located at the minor radius $r_w > a$. [Even though Δ' is usually calculated at marginal stability point $\gamma = 0$, at which a resistive wall does not play a role, but this is not the case if we consider a feedback scheme with complex gains, or when a toroidal plasma flow is present.] The field jump condition across the wall is

$$\left.\frac{r[\psi']}{\psi}\right|_{r_w} = \gamma\tau_w, \quad (6)$$

where $\tau_w = \mu_0 r_w d_w/\eta_w$ is the wall time with d_w and η_w being the wall thickness and resistivity, respectively.

A feedback system requires sensors and active coils. Since we assume a single poloidal harmonic m, both sensor and active coils are "idealized", i.e., measuring/launching a single harmonic magnetic field. We consider three types of sensors, all located at the wall radius r_w. For radial sensors, the sensor signal y is the flux $\psi(r_w)$ at the wall radius. The external poloidal sensors are defined by $y = -r\psi'|_{r_w+}$, i.e., the radial derivative of the flux function just *outside* the resistive wall. The internal poloidal sensors are defined by $y = -r\psi'|_{r_w-}$, i.e., the radial derivative of the flux function just *inside* the resistive wall. In the following, we shall consider two types of active coils, defined by their relative radial location to the wall.

B. External active coils

In this case, the active coils are located outside the wall $r_w < r_f$. In the vacuum region $r_w < r < r_f$, the solution can be written as

$$\psi(r) = \psi_f\left(\frac{r}{r_w}\right)^m + c\left(\frac{r}{r_w}\right)^{-m},$$

where $\psi_f \equiv \psi_f(r_w)$ is the free-space field at the wall radius, produced by the active coil current solely.

Consider a generic feedback controller K, with the (simplified) feedback law for three types of sensors

$$\psi_f = -Ky = -K\begin{cases} \psi_f + c, & \text{radial}-\text{sensor} \\ -m(\psi_f - c), & \text{external}-\text{poloidal}-\text{sensor} \\ -m(\psi_f - c) + \gamma\tau_w(\psi_f + c) & \text{internal}-\text{poloidal}-\text{sensor} \end{cases}.$$

The above feedback law immediately relates the coefficient c to ψ_f

$$c = \psi_f\begin{cases} -(1+K)/K, & \text{radial}-\text{sensor} \\ -(1-mK)/mK, & \text{external}-\text{poloidal}-\text{sensor} \\ -[1-(m-\gamma\tau_w)K]/(m+\gamma\tau_w)K, & \text{internal}-\text{poloidal}-\text{sensor} \end{cases}.$$

The wall jump condition (6) helps us to introduce and calculate a quantity

$$\alpha_e \equiv -\frac{1+\frac{1}{m}\frac{r\psi'}{\psi}\Big|_{r_w-}}{1-\frac{1}{m}\frac{r\psi'}{\psi}\Big|_{r_w-}} = \begin{cases} \dfrac{\gamma\tau_w + 2mK}{\gamma\tau_w + 2m + 2mK}, & \text{radial} \\ \dfrac{\gamma\tau_w + 2m^2K/(1-2mK)}{\gamma\tau_w + 2m + 2m^2K/(1-2mK)}, & \text{external}-\text{poloidal} \\ \dfrac{\gamma\tau_w + 2m^2K}{\gamma\tau_w + 2m - 2m^2K} & \text{internal}-\text{poloidal} \end{cases}.$$

The above quantity α_e, connected with other jump conditions (2) and (3) by the relation (4), yields the same expression for Δ' at the rational surface r_s, as Eq. (5), but with the coefficient B replaced by B_e

$$B_e = \frac{1}{1-\alpha_e a^{2m}/r_w^{2m}} - \frac{m\beta}{2(m-nq_a)^2}.$$

C. Internal active coils

In this case, the active coils are located between the plasma surface and the wall $a < r_f < r_w$. In the vacuum region $r_f < r < r_w$, the field solution can be written as

$$\psi(r) = \psi_f\left(\frac{r}{r_w}\right)^{-m} + c_1\left(\frac{r}{r_w}\right)^{m} + c_2\left(\frac{r}{r_w}\right)^{-m},$$

where $\psi_f \equiv \psi_f(r_w)$ is again the free-space field at the wall radius, produced by the active coil current solely.

The feedback laws become

$$\psi_f = -Ky = -K\begin{cases} \psi_f + c_1 + c_2, & \text{radial}-\text{sensor} \\ m(\psi_f + c_1 + c_2), & \text{external}-\text{poloidal}-\text{sensor} \\ m(\psi_f - c_1 + c_2) & \text{internal}-\text{poloidal}-\text{sensor} \end{cases}.$$

The above feedback equation, together with the wall jump condition (6), determines the coefficients c_1 and c_2

$$c_1 = \psi_f\begin{cases} \gamma\tau_w/2mK, & \text{radial}-\text{sensor} \\ \gamma\tau_w/2m^2K, & \text{external}-\text{poloidal}-\text{sensor} \\ \gamma\tau_w/2mK(m+\gamma\tau_w), & \text{internal}-\text{poloidal}-\text{sensor} \end{cases}$$

$$c_2 = -\psi_f\begin{cases} (\gamma\tau_w + 2m + 2mK)/2mK, & \text{radial}-\text{sensor} \\ (\gamma\tau_w + 2m + 2m^2K)/2m^2K, & \text{external}-\text{poloidal}-\text{sensor} \\ (\gamma\tau_w + 2m + 2mK(m+\gamma\tau_w))/2mK(m+\gamma\tau_w) & \text{internal}-\text{poloidal}-\text{sensor} \end{cases}.$$

In the vacuum region $a < r < r_f$, we have

$$\psi(r) = \alpha_f\psi_f\left(\frac{r}{r_w}\right)^{m} + c_1\left(\frac{r}{r_w}\right)^{m} + c_2\left(\frac{r}{r_w}\right)^{-m},$$

where $\alpha_f \equiv r_w^{2m}/r_f^{2m}$. This allows us to calculate

$$\frac{r\psi'}{\psi}\Big|_{a+} = m\left[1 - \frac{2}{1-\alpha_i a^{2m}/r_w^{2m}}\right],$$

where

$$\alpha_i = \begin{cases} \dfrac{\gamma\tau_w + 2mK\alpha_f}{\gamma\tau_w + 2m + 2mK}, & \text{radial} - \text{sensor} \\ \dfrac{\gamma\tau_w + 2m^2K\alpha_f}{\gamma\tau_w + 2m + 2m^2K}, & \text{external} - \text{poloidal} - \text{sensor} \\ \dfrac{(1+2mK\alpha_f)\gamma\tau_w + 2m^2K\alpha_f}{(1+2mK)\gamma\tau_w + 2m + 2m^2K} & \text{internal} - \text{poloidal} - \text{sensor} \end{cases}.$$

Following the similar coupling procedures as for the external coils, we arrive at the same dispersion relation (5), but with B replaced by B_i

$$B_i = \frac{1}{1 - \alpha_i a^{2m}/r_w^{2m}} - \frac{m\beta}{2(m - nq_a)^2}. \tag{7}$$

D. Modification of Δ' by feedback

Now we investigate the modification of Δ' by magnetic feedback, based on Eq. (5) which is valid for both external and internal feedback coils. For simplicity, we consider a special case without the wall ($\tau_w = 0$), and with a proportional controller with real feedback gain K.

Making additional notations $\hat{\beta} \equiv m\beta/2(m - nq_a)^2, \alpha_w \equiv a^{2m}/r_w^{2m}, \alpha_s \equiv r_s^{2m}/a^{2m}, C \equiv \alpha_s + (1 - \alpha_s)(1 - \hat{\beta})$, it is easy to derive from Eq. (5)

$$\begin{aligned} \delta\Delta' &\equiv \Delta'(K) - \Delta'(K = 0) \\ &= -\frac{2m}{r_s}\frac{\alpha_s}{C}\frac{1}{(1 - \alpha_s) + (1 - \alpha_w\alpha)C}, \end{aligned} \tag{8}$$

where the parameter α depends on the feedback gain, and is associated with different types of the feedback coils and sensors

$$\alpha(K) \equiv \begin{cases} K/(1+K), & \text{ext.coil+rad.sensor} \\ mK/(1 - mK), & \text{ext.coil+pol.sensor} \\ \alpha_f K/(1+K), & \text{int.coil+rad.sensor} \\ \alpha_f mK/(1+mK) & \text{int.coil+pol.sensor} \end{cases}. \tag{9}$$

Notice that in the absence of the wall, the difference between the internal and the external poloidal sensors disappears. Generally, with $\hat{\beta} < 1$, and with the gain values K being not too large, we always have $\delta\Delta' < 0$ for all types of coils and sensors, meaning a stabilizing effect by the magnetic feedback control.

Figures 2(a) and 2(b) show two examples, with $q_0 = 0.95, m = 2, n = 1, r_0 = 0.653a, r_s = 0.9a, r_w = 1.2a$. We assume $r_f = 1.3a$ for external active coils, and $r_f = 1.1a$ for internal coils. Figure 2(a) shows a case with the thermal $\beta = 0.01$, in which the intrinsic Δ' is already negative without feedback. The effect of a proportional feedback action is to bring Δ' into the deeply stable region. Regardless of the types of active coils, the poloidal sensors work more efficiently.

At higher values of β, the intrinsic value of Δ' becomes positive. This case is shown in Fig. 2(b) at $\beta = 0.03$. All four feedback schemes efficiently reduce Δ'. In particular, the combination of external active coils with poloidal sensors fully stabilizes Δ' at rather moderate gain values (with the gain as defined in this study). However, further increase of the gain value (beyond the values shown in Fig. 2(b)) leads to a destabilization. This is because for this specific combination, the parameter α, from Eq. (9), switches sign at sufficiently large K value. For the practical purpose of stabilizing Δ' with feedback, we should always choose the feedback gain below the critical value. The other three cases also lead to full stabilization at large enough gain values. It is interesting to note that, for these three schemes, the stabilization of Δ' saturates at large enough gain values. This is also evident from Eq. (9).

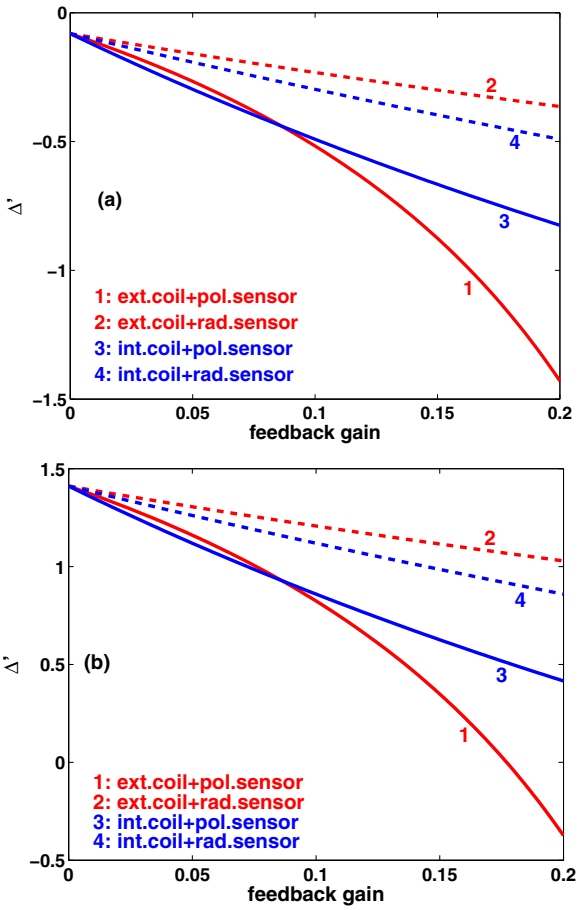

FIG. 2. Stabilizing effect of a simple (proportional) magnetic feedback on the tearing mode stability index Δ', for a cylindrical plasma that is (a) intrinsically stable (with $\beta = 0.01$) and (b) intrinsically unstable (with $\beta = 0.03$). Various types of the feedback coils and sensors are compared.

III. KINETIC MODIFICATION OF Δ'

A. Newcomb-like equation with kinetic effects

Here we derive a Newcomb-like equation, including the drift kinetic modification of the perturbed plasma pressure. Since our eventual goal is to investigate the kinetic effect of trapped particles on Δ', we need to consider a toroidal geometry.

At marginal stability without the equilibrium flow, the perturbed force balance equation reads

$$\nabla \cdot \mathbf{p} = \mathbf{j} \times \mathbf{B} + \mathbf{J} \times \mathbf{b}, \tag{10}$$

where $\mathbf{B}$ and $\mathbf{J}$ are the equilibrium magnetic field and current density, respectively. $\mathbf{b}$ and $\mathbf{j}$ are the corresponding perturbations. $\mathbf{p}$ is the perturbed pressure tensor.

In a torus, the equilibrium magnetic field can be written as the sum of poloidal and toroidal field components

$$\mathbf{B} = \nabla\phi \times \nabla\psi + I(\psi)\nabla\phi, \tag{11}$$

where ϕ is the geometric toroidal angle, ψ is the equilibrium poloidal flux, and $I(\psi)$ is the poloidal current flux function. We define a straight-field-line flux coordinate system (ψ, χ, ϕ), where the poloidal angle χ is chosen such that the jacobian $g = (\nabla\psi \cdot \nabla\chi \times \nabla\phi)^{-1} = qR^2/I$, with $q(\psi)$ being the safety factor and $R(\psi, \chi)$ being the major radius of the torus.

Neglecting the toroidal component of the field perturbation, which is normally small compared to the other two components, we represent the perturbed magnetic field as

$$\mathbf{b} = \nabla\phi \times \nabla\tilde{A},$$

where $\tilde{A}(\psi, \chi, \phi)$ is the toroidal component of the perturbed magnetic vector potential, which will be the solution variable of our final Newcomb equation.

The perturbed pressure tensor $\mathbf{p}$ is derived by solving the drift kinetic equation, as will be shown later on. For the moment, we write $\mathbf{p}$ in a form

$$\mathbf{p} = p\mathbf{I} + p_{||}\hat{\mathbf{b}}\hat{\mathbf{b}} + p_{\perp}(\mathbf{I} - \hat{\mathbf{b}}\hat{\mathbf{b}}),$$

where $\mathbf{I}$ is the identity tensor, $\hat{\mathbf{b}} \equiv \mathbf{B}/B$ is the unit vector of the equilibrium field. The scalar part of the pressure perturbation p represents the adiabatic part of the kinetic pressure, while $p_{||}$ and $p_{\perp}$ represent the parallel and perpendicular components of the non-adiabatic pressure perturbations. All these three components eventually are functions of the solution variable $\tilde{A}$.

Taking the curl-product of the force balance Eq. (10) with $\mathbf{B}/B^2$, and then applying the $\nabla\cdot$ operator, we obtain

$$\nabla \cdot \frac{\mathbf{B}}{B^2} \times (\nabla \cdot \mathbf{p}) = -\mathbf{B} \cdot \nabla \frac{\mathbf{B} \cdot \mathbf{j}}{B^2} + \mathbf{J} \cdot \nabla \frac{\mathbf{B} \cdot \mathbf{b}}{B^2} - \mathbf{b} \cdot \nabla\sigma, \tag{12}$$

where $\sigma \equiv \mathbf{B} \cdot \mathbf{J}/B^2$ characterizes the equilibrium parallel current density, and can be calculated as

$$\sigma = -\left(\frac{dI}{d\psi} + \frac{I}{B^2}\frac{dP}{d\psi}\right),$$

where P is the isotropic equilibrium pressure, satisfying the equilibrium force balance condition $\nabla P = \mathbf{J} \times \mathbf{B}$.

In a general toroidal geometry, the four terms from Eq. (12) can be expressed as follows

$$g\mathbf{b} \cdot \nabla\sigma = \frac{\partial\sigma}{\partial\chi}\frac{\partial\tilde{A}}{\partial\psi} - \frac{\partial\sigma}{\partial\psi}\frac{\partial\tilde{A}}{\partial\chi},$$

$$g\mathbf{J} \cdot \nabla \frac{\mathbf{B} \cdot \mathbf{b}}{B^2} = g\mathbf{J} \cdot \nabla\left[\frac{1}{I^2 + g^{\psi\psi}}\left(g^{\psi\psi}\frac{\partial\tilde{A}}{\partial\psi} + g^{\psi\chi}\frac{\partial\tilde{A}}{\partial\chi}\right)\right],$$

$$\begin{aligned} g\mathbf{B} \cdot \nabla \frac{\mathbf{B} \cdot \mathbf{j}}{B^2} = &\left(\frac{\partial}{\partial\chi} + q\frac{\partial}{\partial\phi}\right)\left\{\frac{I^2}{I^2 + g^{\psi\psi}}\frac{1}{q}\frac{\partial}{\partial\psi}\right. \\ &\times \left[\frac{q}{I}\left(g^{\psi\psi}\frac{\partial\tilde{A}}{\partial\psi} + g^{\psi\chi}\frac{\partial\tilde{A}}{\partial\chi}\right)\right] \\ &+ \frac{I^2}{I^2 + g^{\psi\psi}}\frac{1}{q}\frac{\partial}{\partial\chi}\left[\frac{q}{I}\left(g^{\chi\chi}\frac{\partial\tilde{A}}{\partial\chi} + g^{\psi\chi}\frac{\partial\tilde{A}}{\partial\psi}\right)\right] \\ &\left. - \frac{1}{I^2 + g^{\psi\psi}}\frac{1}{g}\frac{\partial^2\tilde{A}}{\partial\phi\partial\chi}\right\}, \end{aligned}$$

$$\begin{aligned} g\nabla \cdot &\frac{\mathbf{B}}{B^2} \times (\nabla \cdot \mathbf{p}) \\ &= \frac{\partial}{\partial\chi}\left(\frac{I}{B^2}\right)\frac{\partial(p + p_{\perp})}{\partial\psi} - \frac{\partial}{\partial\psi}\left(\frac{I}{B^2}\right)\frac{\partial(p + p_{\perp})}{\partial\chi} \\ &+ \left[\frac{\partial}{\partial\psi}\left(\frac{qg^{\psi\psi}}{IB^2}\right) + \frac{\partial}{\partial\chi}\left(\frac{qg^{\psi\chi}}{IB^2}\right)\right]\frac{\partial(p + p_{\perp})}{\partial\phi} \\ &+ \frac{\partial}{\partial\psi}\left(P + \frac{B^2}{2}\right)\left[\frac{\partial}{\partial\chi}\left(\frac{I}{B^4}p_k\right) - \frac{\partial}{\partial\phi}\left(\frac{qg^{\psi\psi}}{IB^4}p_k\right)\right] \\ &- \frac{\partial}{\partial\chi}\left(\frac{B^2}{2}\right)\left[\frac{\partial}{\partial\psi}\left(\frac{I}{B^4}p_k\right) + \frac{\partial}{\partial\phi}\left(\frac{qg^{\psi\chi}}{IB^4}p_k\right)\right], \end{aligned}$$

where we have introduced a new notation $p_k \equiv p_{||} - p_{\perp}$. The metric elements are defined as $g^{\psi\psi} \equiv |\nabla\psi|^2, g^{\chi\chi} \equiv |\nabla\chi|^2$, $g^{\psi\chi} \equiv \nabla\psi \cdot \nabla\chi$.

We now follow the procedures from Ref. 30, in order to simplify the above expressions. We shall assume $g^{\psi\psi} \ll I^2$, dropping all the $O(B_p^2/B^2)$ terms. Furthermore, we consider a single poloidal and toroidal harmonic for the perturbation $\tilde{A}$, i.e., $\tilde{A} = A(\psi)\exp(im\chi - in\phi)$, with the poloidal mode number m and the toroidal mode number n, respectively. This significantly simplifies the final equation, at the expense of losing the toroidicity induced coupling between poloidal harmonics. Other toroidal effects, such as the trapped particles (which give the key kinetic effects in this study), are fully retained.

Under the above single harmonic assumption, we can easily relate the plasma normal displacement, as well as the scalar pressure term p, to the perturbed flux function A. The scalar product of $\nabla\psi$ with the ideal MHD equation $\mathbf{b} = \nabla \times (\xi \times \mathbf{B})$ gives $\xi \cdot \nabla\psi = -m/(m - nq)A$. The scalar pressure term is expressed as $p = -\xi \cdot \nabla P = m/(m - nq)(dP/d\psi)A$. Note that the equilibrium pressure P here is generally the sum of both thermal and energetic particle pressures. Therefore, the perturbed scalar pressure p includes the adiabatic contributions from both thermal and energetic particles.

The final equation is obtained by multiplying Eq. (12) with $\exp(-im\chi + in\phi)$, and then taking the average over the flux surface, yielding

$$\frac{I}{q}\frac{d}{d\psi}\left(\frac{q}{I}\bar{g}^{\psi\psi}\frac{dA}{d\psi}\right)-m^2\bar{g}^{\chi\chi}A-\frac{m}{m-nq}I\frac{d\bar{\sigma}}{d\psi}A$$
$$-\frac{m^2}{(m-nq)^2}I\frac{d}{d\psi}\left(\frac{\bar{g}}{q}\right)\frac{dP}{d\psi}A-\frac{m}{m-nq}\frac{I}{q}$$
$$\left[\frac{d}{d\psi}\left(\ln\frac{\bar{g}}{q}\right)(gp_\perp)_m-\frac{1}{\bar{B}^2}\frac{d}{d\psi}\left(P+\frac{\bar{B}^2}{2}\right)(gp_k)_m\right]=0, \tag{13}$$

where the surface average $\bar{f}\equiv\int_0^{2\pi}fd\chi/(2\pi)$ is defined for equilibrium quantities. The last term from the left hand side of Eq. (13) represents the drift kinetic contribution to the Newcomb-like equation, in the toroidal geometry. Without this term, Eq. (13) recovers Eq. (26) from Ref. 30 (except for a q factor which is omitted in the fourth term of Eq. (26) in Ref. 30). In deriving Eq. (13), we neglected the terms associated with $g^{\psi\chi}$. The jacobian is attached to the kinetic pressures, for the convenience of deriving the latter (as shown in Sec. III B). We also mention that, by taking the surface average of the momentum balance equation in favor of deriving a single Newcomb-like equation, we lose certain toroidal coupling effects, which can be important as shown in a recent fluid calculation of Δ'.[31] The sideband coupling between the magnetic field line curvature and the perturbed kinetic pressure can also be important. The finite orbit effect (of energetic particles) may enhance this coupling. Finally, the drift kinetic effect itself also enriches the poloidal spectrum of the perturbed kinetic pressures.[33] All these mode coupling effects can generally only be studied numerically, though a three-mode coupling problem, between m and $m\pm1$ harmonics, may still be analytically tractable. This will be examined in a future work.

B. Drift kinetic pressures

Here we derive a compact form that relates the perturbed kinetic pressure terms to the perturbed flux function A, by solving the drift kinetic equations in the limit of vanishing orbit width. We consider contributions from both thermal particles (ions and electrons), and hot ions. Only the magnetic precession drift resonance effect will be included. The full toroidal geometry is retained.

The non-adiabatic part of the drift kinetic pressure terms are calculated as

$$p_{||}=\int Mv_{||}^2\delta f_L dv,\quad p_\perp=\frac{1}{2}\int Mv_\perp^2\delta f_L dv, \tag{14}$$

where M is the particle mass, δf_L is the perturbed distribution function, satisfying the drift kinetic equation[32]

$$\frac{d\delta f_L}{dt}=\frac{\partial f_0}{\partial\varepsilon}\frac{\partial H_L}{\partial t}-\frac{\partial f_0}{\partial P_\phi}\frac{\partial H_L}{\partial\phi}-C(\delta f_L), \tag{15}$$

where f_0 is the equilibrium distribution function of particles, ε is the particle energy, P_ϕ is the particle toroidal canonical momentum, and $C(\delta f_L)$ is the collision operator. H_L is the perturbed particle Lagrangian

$$H_L=Mv_{||}^2\kappa\cdot\xi_\perp+\mu(b_{||}+\nabla B\cdot\xi_\perp),$$

where κ is the equilibrium magnetic field curvature, μ is the magnetic moment, and $b_{||}$ is the parallel component of the perturbed magnetic field. Under the single harmonic approximation for the perturbations, the particle Lagrangian can be expressed in terms of the flux function A

$$H_L=\varepsilon_k\left[C_1\left(\frac{m}{m-nq}A\right)+C_2\frac{d}{d\psi}\left(\frac{q}{m-nq}A\right)+C_3\frac{dA}{d\psi}\right]$$
$$=\varepsilon_k\sum_{k=1}^{3}C_kX_{km},$$

where $\varepsilon_k\equiv Mv^2/2$ is the particle kinetic energy. The equilibrium coefficients C_k are defined as

$$C_1\equiv-\frac{2}{B^2}\left[\left(\frac{1}{2}-\frac{\Lambda}{2h}\right)\frac{dP}{d\psi}+\left(1-\frac{\Lambda}{2h}\right)\frac{\partial B^2}{\partial\psi}\right],$$
$$C_2\equiv-\frac{i}{B^2}\left(1-\frac{\Lambda}{2h}\right)\frac{F}{gB}\frac{\partial B^2}{\partial\chi},\quad C_3\equiv\frac{\Lambda hg^{\psi\psi}}{B_0^2R^2},$$

where $\Lambda\equiv B_0\mu/\varepsilon_k$ is the particle pitch angle, $h\equiv B_0/B$, with B_0 being the equilibrium field amplitude at the magnetic axis. The terms associated with the metric element $g^{\psi\chi}$ are consistently neglected as in the fluid treatment.

With a simplified collision operator $C(\delta f_L)=\nu_{\text{eff}}\delta f_L$, Eq. (15) can be analytically solved.[32] We note that the Krook collision is a simplified assumption that facilitates analytic solution of the drift kinetic equation. Our further study assumes a collisionless plasma. The solution of Eq. (15) is inserted into Eq. (14) to calculate the kinetic pressures. Considering the toroidal magnetic precession drift of trapped particles only, and neglecting the finite banana width effect, the poloidal Fourier harmonics of the perturbed kinetic pressures can be written in the following compact form[33]

$$(gp_{||,\perp})_m=\frac{P_j}{B_0}\sum_{k=1}^{3}\int d\Lambda H_{km}G_m^{||,\perp}I_jX_{km}, \tag{16}$$

where the index j stands for thermal ions (i), thermal electrons (e), or hot ions (h). Following,[33] the "geometrical" factors H_{km} and $G_m^{||,\perp}$ are defined as

$$H_{km}=\frac{e^{inq\chi_L}}{\hat{\tau}_b}\int_{\chi_L}^{\chi_U}\frac{gB}{\sqrt{1-\Lambda/h}}C_k(\chi)e^{i(m-nq)\chi}d\chi,$$

$$G_m^{\perp}=\frac{e^{-inq\chi_L}}{2\pi}\int_{\chi_L}^{\chi_U}\frac{gB\Lambda/(2h)}{\sqrt{1-\Lambda/h}}e^{-i(m-nq)\chi}d\chi,$$

$$G_m^{||}=\frac{e^{-inq\chi_L}}{2\pi}\int_{\chi_L}^{\chi_U}gB\Lambda\sqrt{1-\Lambda/h}e^{-i(m-nq)\chi}d\chi,$$

where χ_L and χ_U are, respectively, the lower and upper turning points of the trapped particle along the poloidal angle χ. $\hat{\tau}_b=2\int_{\chi_L}^{\chi_U}gBd\chi/\sqrt{1-\Lambda/h}$ is the normalized particle bounce time (one period).

The factor I_j from Eq. (16) is obtained as a result of the kinetic integration over the particle energy ε_k. This factor depends on the particle equilibrium distribution, as well as the kinetic resonances between particles and the mode. For

the external ideal solution, we assume that the mode frequency is zero. The magnetic precession drift motion of particles is included in the kinetic resonance. For thermal particles, we assume the Maxwellian equilibrium distribution, which leads to

$$I_{i,e} = -\frac{3}{2}\frac{1}{\hat{\omega}_d}\frac{d\ln P_{i,e}}{d\psi},$$

where $\hat{\omega}_d \equiv \langle\omega_d\rangle/(\varepsilon_k/e)$ is the normalized bounce averaged toroidal precession drift frequency of particles. Both the plasma flow and the collisionality are ignored in the above calculations. These factors can be added into the calculations without principle difficulties, but resulting in much more complicated expressions.

For hot ions, we assume a slowing down distribution $f_0 = C/(\varepsilon_k^{3/2} + \varepsilon_c^{3/2})$ for $0 < \varepsilon_k < \varepsilon_h$, and $f_0 = 0$ for $\varepsilon_k > \varepsilon_h$, where ε_c is the crossover energy proportional to the thermal electron temperature, ε_h is the birth energy of hot ions (3.52 MeV for fusion born α-particles). The factor C in the distribution function can be calculated knowing the hot ion pressure P_h. In the absence of plasma flow, the I_j factor for hot ions can be calculated as[34]

$$I_h = -\frac{3}{2}\frac{1}{\hat{\omega}_d}\left(\frac{d\ln P_h}{d\psi} - \frac{d\ln\varepsilon_h}{d\psi}\right).$$

C. Deeply trapped limit

In full toroidal geometry, the kinetic pressures (16) generally can only be computed numerically. However, for deeply trapped particles, the drift kinetic integrations are analytically tractable. Therefore, we shall consider the kinetic contribution from deeply trapped particles.

In this limit, at each flux surface, the particle pitch angle reaches the maximal value $\Lambda_{\max}$, at a poloidal angle $\chi_0 = \chi_L = \chi_U$. The geometrical factors H_{km} and $G_m^{\|,\perp}$ can be easily evaluated even in a generic torus

$$H_{km}|_{\Lambda_{\max}} = \frac{1}{2}C_k(\chi_0)e^{im\chi_0}, \quad G_m^{\perp}\Big|_{\Lambda_{\max}} = \frac{B_0}{\sqrt{H_0}}\frac{g(\chi_0)}{\sqrt{h(\chi_0)}}e^{-im\chi_0},$$
$$G_m^{\|}\Big|_{\Lambda_{\max}} = 0,$$

where $H_0 \equiv -(\partial^2 h/\partial\chi^2)|_{\chi_0}$. We also obtain

$$C_1(\chi_0) = -\frac{\partial\ln B}{\partial\psi}\Big|_{\chi_0}, \quad C_2(\chi_0) = 0, \quad C_3(\chi_0) = \frac{1}{R^2}\frac{g^{\psi\psi}}{B^2}\Big|_{\chi_0}.$$

Note that $C_3(\chi_0)$ is a $O(B_p^2/B^2)$ term, which we shall neglect.

Interestingly, using the Rosenbluth-Sloan formula,[35] the magnetic precession drift frequency of deeply trapped particles can be easily calculated

$$\hat{\omega}_d|_{\Lambda_{\max}} = \frac{1}{\varepsilon}\frac{\partial\hat{J}_0/\partial\psi}{\partial\hat{J}_0/\partial\varepsilon}\Big|_{\Lambda_{\max}} = -\frac{\partial\ln B}{\partial\psi}\Big|_{\chi_0} = C_1(\chi_0),$$

where $\hat{J}_0 = \oint Mv_{\|}dl$ is the longitudinal invariant of the particle motion.

With the inclusion of the drift kinetic effects from the magnetic precession drift of deeply trapped particles, the final Newcomb-like Eq. (13) takes the following form

$$\frac{I}{q}\frac{d}{d\psi}\left(\frac{q}{I}\bar{g}^{\psi\psi}\frac{dA}{d\psi}\right) - m^2\bar{g}^{\chi\chi}A - \frac{m}{m-nq}I\frac{d\bar{\sigma}}{d\psi}A$$
$$-\frac{m^2}{(m-nq)^2}I\frac{d}{d\psi}\left(\frac{\bar{g}}{q}\right)\frac{dP}{d\psi}A - \frac{m^2}{(m-nq)^2}IK_dA = 0, \quad (17)$$

where

$$K_d \equiv -\frac{3f_{\text{kinetic}}}{4q}\left[\frac{d}{d\psi}\left(\ln\frac{\bar{g}}{q}\right) + \frac{1}{\bar{B^2}}\frac{d}{d\psi}\left(P + \frac{\bar{B^2}}{2}\right)\right]$$
$$\times\frac{1}{\sqrt{H_0}}\frac{g(\chi_0)}{\sqrt{h(\chi_0)}}\sum_j K_j, \quad (18)$$

and

$$K_{i,e} = \frac{dP_{i,e}}{d\psi}, \qquad K_h = \frac{dP_h}{d\psi} - P_h\frac{d\ln\varepsilon_h}{d\psi}. \quad (19)$$

In deriving Eqs. (17) and (18), we have practically assumed a δ-function in pitch angle, $\delta(\Lambda - \Lambda_{\max})$, for the particle equilibrium distribution function. To somewhat relax this assumption, we introduce a fraction coefficient f_{kinetic} in Eq. (18). This coefficient roughly represents the fraction of deeply trapped particles among the total trapped particles, with $f_{\text{kinetic}} = 1$ corresponds to the δ-function distribution in particle pitch angle for deeply trapped particles. Since we expect that those particles, which has a pitch angle Λ sufficiently close to $\Lambda_{\max}$, will make similar contribution to the modification of Δ', as the deeply trapped ones, in practice f_{kinetic} represents the fraction of those particles which are deeply or sufficiently deeply trapped. Without an exact definition for sufficiently deeply trapped particles, we introduce the parameter f_{kinetic}. This parameter also allows us to trace the kinetic contribution to Δ' in the later study. This contribution is excluded by setting $f_{\text{kinetic}} = 0$.

The kinetic contribution from the deeply trapped hot ions has two terms. The second term is proportional to the hot ion pressure (not the pressure gradient). It can be shown that, for the slowing equilibrium distribution which is isotropic in particle pitch angle, a similar term also appears in the adiabatic portion of the perturbed kinetic pressure. But that term is of order ε smaller than that from Eq. (19). Therefore, no full cancellation can occur.

On the other hand, if the hot ion birth energy ε_h is a constant (such as that for fusion born α's), the kinetic contributions from trapped thermal particles and from trapped hot ions cannot be distinguished, in the sense that the ratio of the hot ion pressure to the thermal one does not affect the result, as long as the total (equilibrium) pressure remains the same. This is true only if we neglect the finite orbit width effect of hot ions, which is the approximation adopted in this work.

We note that the last term in the left hand side (LHS) of Eq. (17) represents the non-adiabatic response of deeply trapped particles. The adiabatic response of (all) particles is included in the second last term of the LHS of Eq. (17),

because the equilibrium pressure P includes both thermal and (isotropic) kinetic pressures from hot ions.

We also note that the non-adiabatic kinetic contribution has order β_{th} or β_h, similar to the term due to the fluid pressure gradient. Moreover, these two terms share the same order of singularity near rational surfaces. Therefore, The eventual kinetic modification of Δ' in our model shares the similar physics as that from the fluid pressure gradient, i.e., by changing the Mercier index as shown below.

D. Calculation of Δ'

Equation (17) can be solved for Δ', following the same procedure as that in Ref. 30. In case that the last two pressure terms do not vanish, there are large and small solutions near the rational surface $q(\psi_s) = m/n$. The ratio of the small to large solution is discontinuous across the rational surface. This discontinuity is defined as Δ' and is used as the asymptotic matching parameter to the inner resistive layer solution.

Introducing a local variable X near the rational surface $\psi = \psi_s$

$$X \equiv 2m\left[\left(\frac{\bar{g}^{\chi\chi}}{\bar{g}^{\psi\psi}}\right)^{1/2}\left(\frac{dq}{d\psi}\right)^{-1}\right]_{\psi_s}\left(q-\frac{m}{n}\right).$$

The leading order in the $1/m$ expansion of Eq. (17) gives

$$\frac{d^2A}{dX^2}+\left(-\frac{1}{4}+\frac{-\lambda}{X}+\frac{\frac{1}{4}-D_I}{X^2}\right)A=0, \tag{20}$$

where

$$\lambda = -\frac{qI}{2m}\left(\frac{dq}{d\psi}\right)^{-1}\frac{d\bar{\sigma}}{d\psi}\frac{1}{\sqrt{\bar{g}^{\psi\psi}\bar{g}^{\chi\chi}}}\bigg|_{\psi_s}, \tag{21}$$

$$D_I = \frac{Iq^2}{\bar{g}^{\psi\psi}}\left(\frac{dq}{d\psi}\right)^{-2}\left(\frac{dP}{d\psi}\frac{d}{d\psi}\frac{\bar{g}}{q}+K_d\right)+\frac{1}{4}. \tag{22}$$

Note that the drift kinetic effect modifies Δ' essentially via the modification of the Mercier index D_I.[36] The kinetic modification of the Mercier criteria has been studied in literature, e.g., in Ref. 37 for a large aspect ratio plasma. Our result obtained here is valid for a generic torus, but in the deeply trapped limit. Both in Ref. 37 and here, the kinetic modification is shown to be proportional to the gradient of the equilibrium pressure.

The solution of Eq. (20), which is the Whittaker function,[38] has a power series expansion for small X, when $\nu \equiv -1/2+\sqrt{D_I}$ is not an integer. The two independent solutions, from two sides of the rational surface, which satisfy the inner asymptotic of the outer ideal solution,[30] are

$$A^+(X(r)>0) = (r-r_s)^{-\nu}\left(1-\frac{\lambda}{2\nu}X(r)+\cdots\right) + \Delta_+(r-r_s)^{1+\nu}\left(1+\frac{\lambda}{2(1+\nu)}X(r)+\cdots\right),$$

$$A^-(X(r)<0) = (r_s-r)^{-\nu}\left(1+\frac{\lambda}{2\nu}X(r)+\cdots\right) + \Delta_-(r_s-r)^{1+\nu}\left(1-\frac{\lambda}{2(1+\nu)}X(r)+\cdots\right),$$

where r is an equivalent cylindrical minor radius, and

$$X(r) = 2m\sqrt{\frac{\bar{g}^{\chi\chi}}{\bar{g}^{\psi\psi}}}\frac{d\psi}{dr}\bigg|_{r_s}(r-r_s) \equiv (r-r_s)X_g,$$

$$\Delta_+ = \frac{\Gamma(-1-2\nu)}{\Gamma(1+2\nu)}\frac{\Gamma(1+\lambda+\nu)}{\Gamma(\lambda-\nu)}X_g^{1+2\nu},$$

$$\Delta_- = \frac{\Gamma(-1-2\nu)}{\Gamma(1+2\nu)}\frac{\Gamma(1-\lambda+\nu)}{\Gamma(-\lambda-\nu)}X_g^{1+2\nu}.$$

In a true circular cylinder, $\bar{g}^{\psi\psi} = (d\psi/dr)^2$, and hence $X_g = 2m\sqrt{\bar{g}^{\chi\chi}}$. The asymptotic matching parameter is calculated as

$$\Delta' \equiv \Delta_+ + \Delta_- = -X_g^{1+2\nu}\cos(\lambda\pi)\frac{\sin\nu\pi}{\nu\pi}\frac{\Gamma(1-2\nu)}{\Gamma(2+2\nu)}\Gamma \times (1-\lambda+\nu)\Gamma(1+\lambda+\nu). \tag{23}$$

The above Δ' has a small ν expansion

$$\Delta' = -X_g^{1+2\nu}\lambda\pi\cot(\lambda\pi)\{1+[-2-4\Psi(1) + \Psi(1-\lambda)+\Psi(1+\lambda)]\nu+\cdots\}, \tag{24}$$

where $\Psi(x) \equiv d\ln\Gamma(x)/dx$ is the digamma function. Interestingly as $\nu \to 0$ in Eq. (24), the above Δ' formally recovers the result with vanishing pressure gradient (and in the absence of the kinetic effect) at the rational surface, even though the latter case cannot be derived using the same power series expansion for the solution.

The drift kinetic effects of trapped particles modify Δ' via the parameter $\nu \equiv -1/2+\sqrt{D_I}$, see Eq. (22). It is evident from Eq. (23) that the stability margin occurs at $\lambda = 0.5$, independent of ν. At small values of ν, $0 \le \nu < 0.5$, Δ' is positive (negative) when $\lambda > 0.5$ (< 05). A larger value of ν can change the sign of Δ'.

E. An analytic toroidal equilibrium

In order to quantify, the drift kinetic effect of deeply trapped particles on Δ', we consider an exact analytic toroidal equilibrium with elliptic shaping. The so-called Solov'ev equilibrium[39] is specified by a special choice of the equilibrium pressure and current profiles, as well as the plasma boundary shape. The poloidal current flux function from Eq. (11) is a constant $I(\psi) = const.$ The equilibrium pressure is a linear function of the poloidal flux function ψ

$$P(\psi) = -\frac{I}{R_0^3 q_0}\frac{1+\kappa^2}{\kappa}\psi,$$

where $\kappa(\psi) = const$ is the elongation of the plasma cross section shape. Specifying the plasma boundary as

$$\begin{aligned} R|_{r=a} &= R_0(1+2\varepsilon_a\cos\theta)^{1/2}, \\ Z|_{r=a} &= R_0\varepsilon_a\kappa\sin\theta(1+2\varepsilon_a\cos\theta)^{-1/2}, \end{aligned} \tag{25}$$

where $\varepsilon_a \equiv a/R_0$, the solution of the Grad-Shafranov equation reads

$$\psi = \frac{I\kappa}{2R_0^3 q_0}\left[\frac{R^2Z^2}{\kappa^2} + \frac{1}{4}(R^2-R_0^2)^2 - a^2R_0^2\right] = \frac{R_0\kappa I}{2q_0}(\varepsilon_r^2-\varepsilon_a^2),$$

with

$$\begin{aligned} R &= R_0(1+2\varepsilon_r\cos\theta)^{1/2}, \\ Z &= R_0\kappa\varepsilon_r\sin\theta(1+2\varepsilon_r\cos\theta)^{-1/2}, \end{aligned}$$

and $\varepsilon_r \equiv r/R_0$. This series of equilibria is fully specified by five free parameters $(\varepsilon_a, q_0, \kappa, R_0, I)$. Because of the special choice for the plasma shape functions, there is also certain triagularity to the plasma shape (as shown for example in Fig. 3), making this family of equilibria very useful in approximating realistic tokamak plasmas. The only limitation is that the aspect ratio cannot be smaller than 2, constrained by the specification of the plasma boundary (25).

All the equilibrium quantities can be calculated analytically, for instance

$$q = \frac{2q_0}{\pi}\frac{\sqrt{1+2\varepsilon_r}}{1-4\varepsilon_r^2}E(k),$$

$$B^2 = \frac{I^2}{R_0^2}\left[\frac{1}{1+2\varepsilon_r\cos\theta} + \frac{\varepsilon_r^2}{q_0^2}\sin^2\theta + \frac{\kappa^2\varepsilon_r^2}{q_0^2}\left(\frac{\varepsilon_r+\cos\theta+\varepsilon_r\cos^2\theta}{1+2\varepsilon_r\cos\theta}\right)^2\right],$$

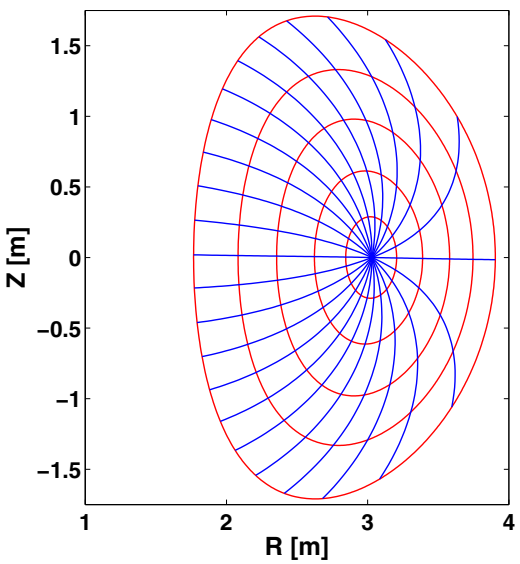

FIG. 3. One toroidal Solov'ev equilibrium shown in a straight field line coordinate system, with $R_0 = 3\text{m}$, $a/R_0 = 0.33, q_0 = 1.4, \kappa = 1.6$.

where $E(k)$ is the complete elliptic integral of the second kind, with $k \equiv \sqrt{4\varepsilon_r/(1+2\varepsilon_r)}$.

Since the derivations of the Newcomb-like equation have been made for a straight field line flux coordinate system with the jacobian $g = qR^2/I$, we need to choose a poloidal angle χ, for the Solov'ev equilibrium, which gives the same jacobian. [The flux system (r,θ,ϕ), with the geometrical angle θ, gives a jacobian $g_{\text{geom}} = R_0^3\kappa\varepsilon_r/R$.] It can be shown that, at each flux surface, the poloidal angle χ should be chosen to satisfy the following equation:

$$\frac{\partial\chi}{\partial\theta} = \frac{R_0^3}{R^3}\frac{q_0}{q}.$$

Defining $\chi = 0$ at $\theta = 0$ (the outboard mid-plane), it is easy to show that χ varies from 0 to 2π, as θ varies from 0 to 2π. All the equilibrium quantities, which enter into the final Newcomb-like equation (17), can also be calculated in the (ψ,χ,ϕ) coordinate system

$$g^{\psi\psi}(\varepsilon_r,\chi(\theta)) = \left(\frac{I\varepsilon_r}{q_0}\right)^2[\sin^2\theta(1+2\varepsilon_r\cos\theta) + \kappa^2(\varepsilon_r+\varepsilon_r\cos^2\theta+\cos\theta)^2(1+2\varepsilon_r\cos\theta)^{-1}],$$

$$g^{\chi\chi} = \left(\frac{q_0}{R_0\kappa\varepsilon_r q}\right)^2[\cos^2\theta(1+2\varepsilon_r\cos\theta)^{-2} + \kappa^2\sin^2\theta(1+\varepsilon_r\cos\theta)^2(1+2\varepsilon_r\cos\theta)^{-4}],$$

$$\sigma = \frac{1+\kappa^2}{\kappa R_0^3 q_0}\frac{I^2}{B^2}.$$

Some of the intermediate quantities, appearing during the previous derivations, can also be analytically calculated. In particular, the normalized bounce period $\hat{\tau}_b$, the normalized toroidal magnetic precession frequency $\hat{\omega}_d$, for deeply trapped particles, as well as some other factor from Eq. (18), are

$$\hat{\tau}_b|_{\Lambda_{\max}} = 2\pi q_0 R_0 I\left(\frac{1}{1+2\varepsilon_r}+\frac{\kappa^2\varepsilon_r^2}{q_0^2}\right) \times\left[\frac{\varepsilon_r}{2(1+2\varepsilon_r)}+\frac{\kappa^2\varepsilon_r^3}{q_0^2}+\frac{(1-\kappa^2)\varepsilon_r^2}{2q_0^2}(1+2\varepsilon_r)\right]^{-1/2},$$

$$\hat{\omega}_d|_{\Lambda_{\max}} = \frac{q_0}{R_0\kappa\varepsilon_r I}\left(\frac{1}{1+2\varepsilon_r}+\frac{\kappa^2\varepsilon_r^2}{q_0^2}\right)^{-1}\left[\frac{1}{(1+2\varepsilon_r)^2}-\frac{\kappa^2\varepsilon_r}{q_0^2}\right],$$

$$g(\chi_0) = \frac{R_0^2 q}{I}(1+2\varepsilon_r),$$

$$h(\chi_0) = \left(\frac{1}{1+2\varepsilon_r}+\frac{\kappa^2\varepsilon_r^2}{q_0^2}\right)^{-1/2},$$

$$H_0 = \left(\frac{1}{1+2\varepsilon_r}+\frac{\kappa^2\varepsilon_r^2}{q_0^2}\right)^{-3/2} \times\left[\frac{\varepsilon_r}{2(1+2\varepsilon_r)}+\frac{\kappa^2\varepsilon_r^3}{q_0^2}+\frac{(1-\kappa^2)\varepsilon_r^2}{2q_0^2}(1+2\varepsilon_r)\right].$$

Some of the surface averaged equilibrium quantities involve lengthy calculations (see Appendix), but can be eventually expressed in terms of the complete elliptic integrals of the first ($K(k)$) and second ($E(k)$) kind

$$\bar{g}^{\psi\psi} = \frac{1}{2\pi}\int_0^{2\pi} g^{\psi\psi} d\chi = \frac{1}{2\pi}\int_0^{2\pi} g^{\psi\psi}\frac{\partial\chi}{\partial\theta}d\theta = \frac{1+\kappa^2}{3\pi q_0 q} I^2\sqrt{1+c}[E-(1-c)K],$$

$$\bar{g}^{\chi\chi} = \frac{4}{15\pi R_0^2\kappa^2 c^4}\left(\frac{q_0}{q}\right)^3\frac{\sqrt{1+c}}{(1-c^2)^4}\{2(1-c^2)[(-2+19c^2+15c^4)E+2(1-c)(1-5c^2)K] + \frac{\kappa^2}{21}[(44+279c^2-258c^4+63c^6)E+(1-c)(-44+3c^2+9c^4)K]\},$$

$$\bar{g} = \frac{q}{I}\bar{R^2} = \frac{2R_0^2 q_0}{\pi I\sqrt{1+c}}K,$$

$$\bar{B^2} = \frac{I^2}{\pi R_0^2}\frac{q_0}{q}\sqrt{1+c}\left\{\frac{2}{3}(1-c^2)^{-2}[4E-(1-c)K] - \frac{1}{q_0^2}[E-(1+c)^{-1}K] + \frac{\kappa^2}{15q_0^2}(1-c^2)^{-1}\times[(1+3c^2)E-(1-c)K]\right\},$$

where $c \equiv 2\varepsilon_r$.

The exact analytic expression for the surface averaged parallel current density $\bar{\sigma}$ is difficult to calculate. An approximate expression, up to the fourth order accuracy in ε, can be obtained

$$\bar{\sigma} \simeq \frac{1}{2\pi R_0 q}\frac{1+\kappa^2}{\kappa}\times\left(\sigma_1+\frac{1}{q_0^2}\sigma_2+\frac{1}{q_0^4}\sigma_3+\frac{\kappa^2}{q_0^2}\sigma_4+\frac{\kappa^2}{q_0^4}\sigma_5+\frac{\kappa^4}{q_0^4}\sigma_6\right),$$

where

$$\sigma_1 = 4(1+c)^{-1/2}K,$$

$$\sigma_2 = \frac{2}{15}(1+c)^{1/2}[-(1+3c^2)E+(1-c)K],$$

$$\sigma_3 = \frac{1}{315}(1+c)^{1/2}[(-4+15c^2+21c^4)E + 4(1-c)(1-3c^2)K],$$

$$\sigma_4 = \frac{1}{315}(1+c)^{1/2}[(86-270c^2+21c^4)E - 2(1-c)(43-24c^2)K],$$

$$\sigma_5 = \frac{1}{315}(1+c)^{1/2}[(8-9c^2+21c^4)E - (1-c)(8-3c^2)K],$$

$$\sigma_6 = \frac{4}{315}(1+c)^{1/2}[-(16+24c^2-147c^4)E + 4(1-c)(4+9c^2)K].$$

Numerical test shows that the above approximation results in less than 1% error for all reasonable choices of equilibrium parameters.

The analytic coefficients, calculated for the Solov'ev equilibrium, can be directly inserted into Eqs. (21)–(23), for computing Δ'. By varying the q_0 value, it is also possible to fix the radial location of the rational surface, say at $\varepsilon_r = 1/6$, giving $k = \sqrt{2}/2$, where the values of the elliptic integrals E and K are known, and hence the above analytic derivations can be further advanced. We shall, however, stay with more generic cases, by numerically evaluating equilibrium quantities at arbitrary radial location, for the rational surface. It can be verified that the parameters λ and ν, from Eqs. (21) and (22), respectively, are dimensionless (independent of R_0 and I), as expected.

As examples, we show quantitative results for the above series of Solov'ev equilibria, with $a/R_0 = 0.33, R_0 = 3\text{m}$, and varying q_0 and κ. Figure 4 shows three q-profiles, with the on-axis value $q_0 = 1.2, 1.4$, and 1.6, respectively. [With a given q_0, the q-profile does not depend on the elongation κ.] We vary the kinetic fraction parameter f_{kinetic} from Eq. (18), in order trace the change in Δ', as shown in Fig. 5. In the absence of the kinetic effect ($f_{\text{kinetic}} = 0$), Δ' is positive for all three cases. The kinetic terms destabilize Δ', for cases with $q_0 = 1.2$ and 1.4. However, for the $q_0 = 1.6$ case, which has a large positive Δ' at $f_{\text{kinetic}} = 0$, the kinetic effect

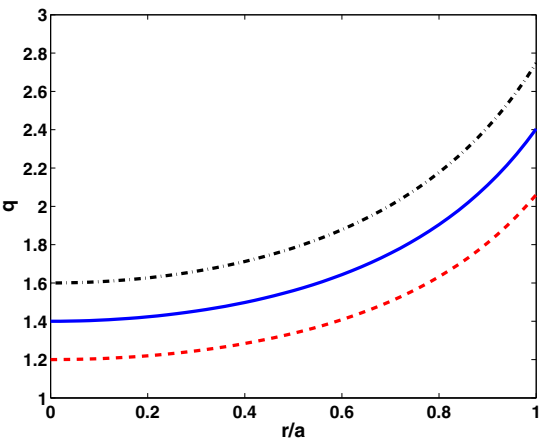

FIG. 4. Radial profiles of the safety factor q, with $q_0 = 1.2, 1.4$, and 1.6, for Solov'ev equilibria with the inverse aspect ratio $a/R_0 = 0.33$.

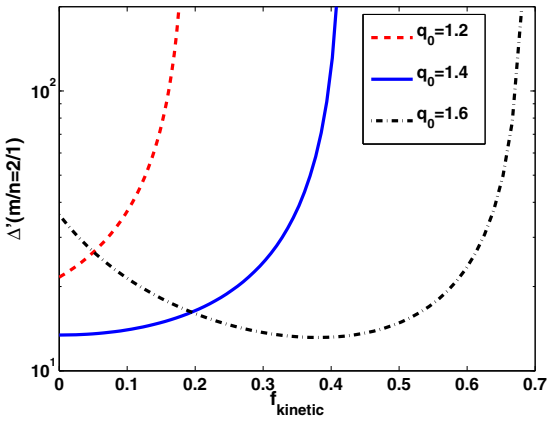

FIG. 5. Calculated Δ' versus the fraction of the drift kinetic contribution from deeply trapped particles, for three toroidal Solov'ev equilibria, with $q_0 = 1.2, 1.4$, and 1.6, respectively. These equilibria have $a/R_0 = 0.33$, $\kappa = 1.6$.

first stabilizes Δ', with a subsequent destabilization at sufficiently large f_{kinetic}.

Further increase of f_{kinetic} leads to an infinite Δ' for all three cases, corresponding to the transition to the ideal instability.[28,40] This transition is associated with the parameter ν approaching 1/2, which is the pole of Δ' (23). The dependence of ν, as well as λ and D_I, as a function of the kinetic fraction parameter is shown in Fig. 6 for $a/R_0 = 0.33$. Note that for this family of Solov'ev equilibria, the values of ν and D_I are independent of q_0 and κ. The current drive term λ does depend on q_0 and κ, but not on f_{kinetic}.

The decrease of the Mercier term D_I, and hence the ν parameter, with f_{kinetic} is due to the cancellation between the two terms $(dP/d\psi)[d(\bar{g}/q)/d\psi]$ and K_d from Eq. (22). For the Solov'ev equilibria, the first (fluid) term is positive, the second (kinetic) is negative. This is easier to see in the large aspect ratio limit for the Solov'ev equilibrium. Keeping only the lowest order terms in ε_r, it can be shown that Eqs. (21) and (22) become

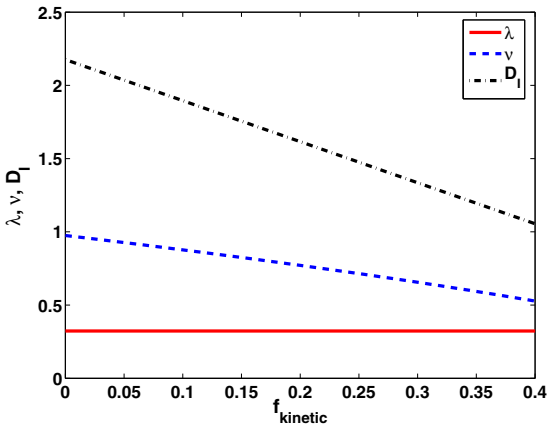

FIG. 6. The current drive term λ, the Mercier index D_I, and the power $\nu = -1/2 + \sqrt{D_I}$ of the large solution, versus the fraction of the drift kinetic contribution from deeply trapped particles, for a toroidal Solov'ev equilibria with $a/R_0 = 0.33, \kappa = 1.6$, and $q_0 = 1.4$.

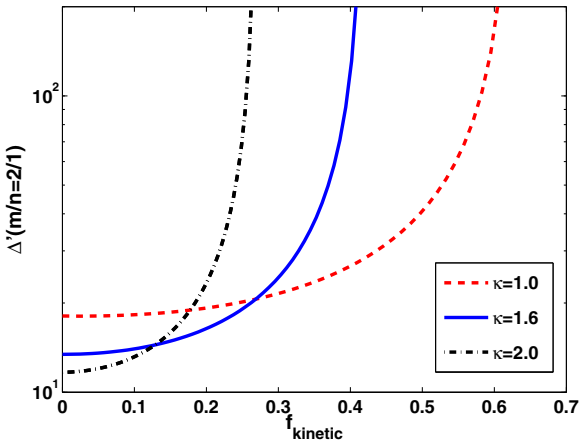

FIG. 7. Calculated Δ' versus the fraction of the drift kinetic contribution from deeply trapped particles, for three toroidal Solov'ev equilibria, with elongation $\kappa = 1, 1.6$, and 2, respectively. These equilibria have $a/R_0 = 0.33, q_0 = 1.4$.

$$\lambda \simeq \frac{8}{15m}\left[\frac{3}{2} + \frac{1+\kappa^2}{4q_0^2}\right],$$
$$D_I \simeq \hat{D}_I(1+\hat{K}_d) + \frac{1}{4}, \quad \hat{D}_I \equiv \frac{16}{75}\frac{1}{\varepsilon_r^2},$$
$$\hat{K}_d \equiv -\frac{f_{\text{kinetic}}}{2\sqrt{2}}\left[\frac{1}{2} + \frac{1+\kappa^2}{4q_0^2}\right]\frac{1}{\sqrt{\varepsilon_r}}. \tag{26}$$

The above asymptotics also qualitatively explain why a smaller value of q_0 leads to ideal marginal stability at a smaller f_{kinetic}, as shown in Fig. 5.

Figure 6 shows that the destabilization of Δ' occurs in the parameter space of $\lambda < 0.5$ and $\nu > 0.5$. This corresponds to the plasma regime, where Δ' is positive in the absence of the kinetic terms yet the ideal mode is table ($\Delta' < \infty$), for these Solov'ev equilibria.

The above results are not very sensitive to the elongation parameter κ, as shown by Fig. 7, where we consider three values of $\kappa = 1, 1.6$, and 2, while fixing $q_0 = 1.4$. For all three κ values, the drift kinetic effects from deeply trapped particles destabilize Δ', till reaching the ideal instability boundary ($\Delta' \to \infty$). Moreover, a stronger elongation requires a smaller kinetic fraction, in order to reach the ideal marginal stability. This again can be understood from the asymptotic formula (26), showing a larger kinetic cancellation of the fluid D_I, at a larger value of κ.

IV. SUMMARY AND DISCUSSION

Based on analytically tractable cases, this work shows two possible mechanisms of modifying Δ', by invoking either the kinetic physics or the active control using magnetic coils.

In the single (poloidal) mode cylindrical approximation, we have shown that the active magnetic control can be effective in modifying Δ', hence the tearing mode stability. Various combinations of types of active and sensor coils can be used, either bringing an intrinsically negative Δ' to a more stable domain, or stabilizing an intrinsically unstable Δ' by the feedback system. This theory may be applied to interpret

the experimental results in RFX,[4] where the internal resonant modes are efficiently suppressed by magnetic feedback coils.

We have investigated drift kinetic effects from trapped particles on Δ'. This requires consideration of toroidal geometry, as well as the inclusion of kinetic pressure tensor terms into the fluid equations. For deeply trapped particles (both thermal and energetic), it is possible to derive a Newcomb-like equation. One simplification in this derivation is the neglect of the finite orbit width (of energetic particles). The eventual calculation of Δ' from the Newcomb equation follows standard procedures.

For a family of toroidal equilibria, all the equilibrium quantities entering the toroidal Newcomb equation can be analytically calculated, which allows us to quantify the modification of Δ' by trapped particle kinetic effects in toroidal geometry. We find that the kinetic contribution tends to reduce the degree of singularity of the large solution from the outer region. As a consequence, the kinetic contribution generally destabilizes Δ', and can lead to the marginal stability for ideal mode. The main physics of the kinetic modification of Δ' in our model comes from the change of the Mercier index due to the non-adiabatic response of deeply trapped particles. Note that the adiabatic response is also included in our model, via the total equilibrium pressure term. This kinetic destabilization effect may partially explain the recent numerical results with NIMROD[27] and M3D-K,[26] although the finite orbit width effect is also included in these numerical studies, which probably also contributes to the kinetic destabilization of Δ'.

Finally, we emphasize that the effects such as the toroidal coupling of different harmonics, the kinetic contributions from other particles rather than deeply trapped ones, and the finite orbit width of energetic particles can potentially also be important for Δ'. We neglected them in this study in favor of analytic tractability. Generally these effects can only be numerically studied.

ACKNOWLEDGMENTS

YQL acknowledges very helpful discussions with Dr. C.G. Gimblett. This work was funded by the RCUK Energy Programme under grant EP/I501045 and the European Communities under the contract of Association between EURATOM and CCFE. The views and opinions expressed herein do not necessarily reflect those of the European Commission.

APPENDIX: A FAMILY OF INTEGRALS

The surface average of equilibrium quantities for the Solov'ev equilibrium involves calculating a family of integrals of the form

$$S_\nu(\lambda) = \int_0^{2\pi} (1+\lambda\cos\theta)^\nu d\theta,$$

where ν is a half integer, and $0 \le \lambda \le 1$.

For $\nu = -1/2$ and $1/2$, the above integral is easily converted to the complete elliptic integrals of the first and second kinds, respectively

$$S_{-1/2} = 4(1+\lambda)^{-1/2}K(k), \quad S_{1/2} = 4\sqrt{1+\lambda}E(k),$$

where $k^2 = 2\lambda/(1+\lambda)$. The integrals for $\nu = -3/2, -5/2, \cdots$, can be calculated using a recursive formula

$$S_{\nu-1} = S_\nu - \frac{\lambda}{\nu}\frac{dS_\nu}{d\lambda}, \tag{A1}$$

valid for arbitrary ν value. For example

$$S_{-3/2} = 4\sqrt{1+\lambda}(1-\lambda^2)^{-1}E,$$

$$S_{-5/2} = \frac{4}{3}\sqrt{1+\lambda}(1-\lambda^2)^{-2}[4E-(1-\lambda)K],$$

$$S_{-7/2} = \frac{4}{15}\sqrt{1+\lambda}(1-\lambda^2)^{-3}[(23+9\lambda^2)E-8(1-\lambda)K],$$

$$S_{-9/2} = \frac{4}{105}\sqrt{1+\lambda}(1-\lambda^2)^{-4}[16(11+13\lambda^2)E - (1-\lambda)(71+25\lambda^2)K],$$

$$S_{-11/2} = \frac{4}{315}\sqrt{1+\lambda}(1-\lambda^2)^{-5}[(563+1338\lambda^2+147\lambda^4)E - 8(1-\lambda)(31+33\lambda^2)K].$$

For $\nu = 3/2, 5/2, \cdots$, the integrals can in principle be calculated by solving the above differential equation (A1), or simply by using the following relation:

$$S_\nu S_{-\nu-1}^{-1} = (1-\lambda)^{\nu+1/2},$$

valid again for arbitrary ν.

[1]R. J. La Haye, Phys. Plasmas **13**, 055501 (2006).
[2]R. Aymar, P. Barabaschi, and Y. Shimomura, Plasma Phys. Controlled Fusion **44**, 519 (2002).
[3]D. F. Escande, R. Paccagnella, S. Cappello, C. Marchetto, and F. D'Angelo, Phys. Rev. Lett. **85**, 3169 (2000).
[4]P. Martin, L. Apolloni, M. E. Puiatti, J. Adamek, M. Agostini, A. Alfier, S. V. Annibaldi, V. Antoni, F. Auriemma, O. Barana, M. Baruzzo, P. Bettini, T. Bolzonella, D. Bonfiglio, F. Bonomo, M. Brombin, J. Brotankova, A. Buffa, P. Buratti, A. Canton, S. Cappello, L. Carraro, R. Cavazzana, M. Cavinato, B. E. Chapman, G. Chitarin, S. Dal Bello, A. De Lorenzi, G. De Masi, D. F. Escande, A. Fassina, A. Ferro, P. Franz, E. Gaio, E. Gazza, L. Giudicotti, F. Gnesotto, M. Gobbin, L. Grando, L. Guazzotto, S. C. Guo, V. Igochine, P. Innocente, Y. Q. Liu, R. Lorenzini, A. Luchetta, G. Manduchi, G. Marchiori, D. Marcuzzi, L. Marrelli, S. Martini, E. Martines, K. McCollam, S. Menmuir, F. Milani, M. Moresco, L. Novello, S. Ortolani, R. Paccagnella, R. Pasqualotto, S. Peruzzo, R. Piovan, P. Piovesan, L. Piron, A. Pizzimenti, N. Pomaro, I. Predebon, J. A. Reusch, G. Rostagni, G. Rubinacci, J. S. Sarff, F. Sattin, P. Scarin, G. Serianni, P. Sonato, E. Spada, A. Soppelsa, S. Spagnolo, M. Spolaore, G. Spizzo, C. Taliercio, D. Terranova, V. Toigo, M. Valisa, N. Vianello, F. Villone, R. B. White, D. Yadikin, P. Zaccaria, A. Zamengo, P. Zanca, B. Zaniol, L. Zanotto, E. Zilli, H. Zohm, and M. Zuin, Nucl. Fusion **49**, 104019 (2009).
[5]S. M. Mahajan, R. D. Hazeltine, H. R. Strauss, and D. W. Ross, Phys. Fluids **22**, 2147 (1979).
[6]H. P. Furth, J. Killeen, and M. N. Rosenbluth, Phys. Fluids **6**, 459 (1963).
[7]P. H. Rutherford, Phys. Fluids **16**, 1903 (1973).
[8]R. Fitzpatrick, Phys. Plasmas **2**, 825 (1995).
[9]H. R. Wilson, J. W. Connor, R. J. Hastie, and C. C. Hegna, Phys. Plasmas **3**, 248 (1996).
[10]H. Zohm, Phys. Plasmas **4**, 3433 (1997).
[11]C. C. Hegna and J. D. Callen, Phys. Plasmas **4**, 2940 (1997).

[12]A. M. Popov, R. J. La Haye, Y. Q. Liu, M. Murakami, N. N. Popova, and A. D. Turnbull, Phys. Plasmas **9**, 4229 (2002).
[13]F. A. G. Volpe, M. E. Austin, R. J. La Haye, J. Lohr, R. Prater, E. J. Strait, and A. S. Welander, Phys. Plasmas **16**, 102502 (2009).
[14]M. Maraschek, G. Gantenbein, Q. Yu, H. Zohm, S. Gnter, F. Leuterer, and A. Manini (ECRH Group, ASDEX Upgrade Team), Phys. Rev. Lett. **98**, 025005 (2007).
[15]A. Isayama and the JT-60 Team, Phys. Plasmas **12**, 056117 (2005).
[16]E. Lazzaro and M. F. F. Nave, Phys. Fluids **31**, 1623 (1988).
[17]A. W. Morris, T. C. Hender, J. Hugill, P. S. Haynes, P. C. Johnson, B. Lloyd, D. C. Robinson, C. Silvester, S. Arshad, and G. M. Fishpool, Phys. Rev. Lett. **64**, 1254 (1990).
[18]D. L. Nadle, C. Cates, H. Dahi, M. E. Mauel, D. A. Maurer, S. Mukherjee, G. A. Navratil, M. Shilov, and E. D. Taylor, Nucl. Fusion **40**, 1791 (2000).
[19]J. M. Finn, Phys. Plasmas **13**, 082504 (2006).
[20]R. D. Hazeltine, D. Dobrott, and T. S. Wang, Phys. Fluids **18**, 1778 (1975).
[21]J. W. Connor and R. J. Hastie, Phys. Fluids **19**, 1727 (1976).
[22]M. Rosenberg, R. R. Dominguez, W. Pfeiffer, and R. E. Waltz, Phys. Fluids **23**, 2022 (1980).
[23]X. S. Lee, S. M. Mahajan, and R. D. Hazeltine, Phys. Fluids **23**, 599 (1980).
[24]M. Zabiégo and X. Garbet, Phys. Plasmas **1**, 1890 (1994).
[25]H. Cai, S. Wang, Y. Xu, J. Cao, and D. Li, Phys. Rev. Lett. **106**, 075002 (2011).
[26]H. Cai and G. Fu, Phys. Plasmas **19**, 072506 (2012).
[27]D. P. Brennan, C. C. Kim, and R. J. La Haye, Nucl. Fusion **52**, 033004 (2012).
[28]W. A. Newcomb, Ann. Phys. (N.Y.) **10**, 232 (1960).
[29]A. Bondeson and H. X. Xie, Phys. Plasmas **4**, 2081 (1997).
[30]C. C. Hegna and J. D. Callen, Phys. Plasmas **1**, 2308 (1994).
[31]C. J. Ham, J. W. Connor, S. C. Cowley, C. G. Gimblett, R. J. Hastie, T. C. Hender, and T. J. Martin, Plasma Phys. Controlled Fusion **54**, 025009 (2012).
[32]F. Porcelli, R. Stankiewicz, W. Kerner, and H. L. Berk, Phys. Plasmas **1**, 470 (1994).
[33]Y. Liu, M. S. Chu, I. T. Chapman, and T. C. Hender, Phys. Plasmas **15**, 112503 (2008).
[34]Y. Liu, M. S. Chu, W. F. Guo, F. Villone, R. Albanese, G. Ambrosino, M. Baruzzo, T. Bolzonella, I. T. Chapman, A. M. Garofalo, C. G. Gimblett, R. J. Hastie, T. C. Hender, G. L. Jackson, R. J. La Haye, M. J. Lanctot, Y. In, G. Machiori, M. Okabayashi, R. Paccagnella, M. Furno Palumbo, A. Pironti, H. Reimerdes, G. Rubinacci, A. Soppelsa, E. J. Strait, S. Ventre, and D. Yadykin, Plasma Phys. Controlled Fusion **52**, 104002 (2010).
[35]M. N. Rosenbluth and M. L. Sloan, Phys. Fluids **14**, 1725 (1971).
[36]C. Mercier, Nucl. Fusion **1**, 47 (1960).
[37]F. Porcelli and M. N. Rosenbluth, Plasma Phys. Controlled Fusion **40**, 481 (1998).
[38]E. T. Whittaker and G. N. Watson, *A Course in Modern Analysis*, 4th ed. (Cambridge University Press, Cambridge, England, 1990).
[39]L. Solov'ev, Zh. Eksp. Teor. Fiz. **53**, 626 (1967).
[40]A. Pletzer, A. Bondeson, and R. L. Dewar, J. Comp. Phys. **115**, 530 (1994).